ELSEVIER

Journal of Physics and Chemistry of Solids 64 (2003) 2147–2156

JOURNAL OF PHYSICS AND CHEMISTRY OF SOLIDS

www.elsevier.com/locate/jpcs

Prediction of lattice constant in perovskites of $GdFeO_3$ structure

Li Chonghe[a], Thing Yihao[b], Zeng Yingzhi[a], Wang Chunmei[a], Wu Ping[a,*]

[a]*Institute of High Performance Computing, 1 Science Park Road, 01-01 The Capricorn, Singapore Science Park II, Singapore, Singapore 117528*

[b]*Department of Materials, National University of Singapore, Lower Kent Ridge Road, Singapore, Singapore 119260*

Received 10 March 2003; accepted 17 April 2003

Abstract

Lattice constants in $GdFeO_3$-type ABO_3 perovskites are correlated to their constituent elemental properties by using linear regression (LR) and artificial neural networks (ANN) techniques and a sample set of 157 known $GdFeO_3$-type ABO_3 perovskites. LR models are first obtained using two elemental ionic radii only and ANN models, using five elemental properties; ionic radii, electronegativities of cation A and B, and the valence of ion A, are further developed to improve the model predictability, which reaches an error limits of less than 2%. It is shown that lattice constants of these compounds only roughly correlate to their ionic radii, and for a good prediction model 3 more elemental properties (electronegativity and valence) are necessary. In new materials research, where lattice constant is one of the key design target, the developed LR and ANN models may be used to screen and shortlist promising perovskites from a large pool of all possible candidates. These selected compounds may undergo further test using relatively more expensive experiments or quantum mechanics computations.

1. Introduction

Perovskite structure, named after the mineral perovskite, $CaTiO_3$, is one of the structure types that are most often encountered in solid state inorganic chemistry [1]. The structure contains a huge variety of compounds, e.g. most of the metallic ions in the periodic table can form a perovskite structure. Due to the non-stoichiometry of the cation and/or the anion, the distortion of the cation configuration, and mixed valence and the valence mixture electronic structure, perovskites have a broad and diverse range of useful physical properties. For instance, it was reported [2] recently that $SrTiO_3$ pervovskite can be used as buffer layer for the direct growth of GaAs on Si substrates.

An ideal perovskite structure belongs to the cubic space group Pm3m. There are also tetragonal, orthorhombic, rhombohedral, monoclinic, and triclinic perovskites which are resulted from the structure deviations of the ideal cubic structure through the tilting of the BO_6 octahedra [3]. Among all the orthorhombically distorted perovskites, $GdFeO_3$-type, named after the orthorhombic $GdFeO_3$ ($a_0 = 5.346$Å, $b_0 = 5.616$Å, $c_0 = 7.668$Å, $Z = 4$, and space group Pbnm [4]), is the most commonly occurred structure and accounts for about 60% of all perovskites. For instance, most $Re^{3+}M^{3+}O_3$ compounds possess this structure, where Re represents the rare earth elements and M represents elements of Mn, Fe, Cr, Al, Ga, V and Ti.

Lattice constant is one of the most critical parameters in materials design, especially for interface applicants. Currently, the considerable lattice mismatch between available substrate and thin films is limiting the fabricate capability for large and defects free III–V semiconductors by molecular beem epitaxy. Better lattice matched substrates or buffer materials are in demand to overcome the manufactory difficulties [2,5]. In this regard, a fast and reliable solution to predict lattice constant for a large

* Corresponding author. Tel.: +65-6419-1212.
E-mail address: wuping@ihpc.a-star.edu.sg (P. Wu).

0022-3697/03/$ - see front matter © 2003 Elsevier Ltd. All rights reserved.
doi:10.1016/S0022-3697(03)00209-9

number of unknown compounds becomes the winning edge in high technology development. Often, there are two broad methods to determine the crystal structure of unknown compounds. The first method is by using X-ray, neutron or electron diffraction, and the other is by theoretical or empirical models. The first method is usually a complicated, difficult and time-consuming job. Single-crystal structure analysis by X-ray, neutron or electron diffraction is a powerful and widely used method for structure determination. However, it is very difficult if not impossible to prepare the form of single crystals of sufficient size and quality for conventional single-crystal X-ray diffraction studies for many important crystalline materials [6,7].

On the other hand, mathematical model prediction of crystal structure has gained increasing attention. By a bond-valence method, Lufaso and Woodward [1] recently developed a software package—SpuDS, which can be used to predict crystal structures merely from the chemical stoichiometry of the perovskite, although the model prediction error can be as high as 4, 2 and 4%, respectively, for the lattice constant a, b and c.

In the present study, an atomic parameter—pattern recognition (PR) or atomic parameter—artificial neural network (ANN) method is adopted, which has been incorporated in an in-house developed pattern recognition/artificial intelligence software tool, APEX [8]. Over the past years, this method has been used to investigate the phase stability and melting behaviour of some binary intermetallic compounds [9–11]. It was also used to predict unknown intermediate compounds and their stoichiometry, melting behaviours, liquids and even simple phase diagrams for some binary molten salt systems [12,13]. In addition, this method was also used in the design of new semiconductors [14,15], new hydrogen storage alloy [16,17] and new additives for galvanizing process [18,19].

We extend the above-mentioned method to study the regularities of lattice constants a, b, and c in $GdFeO_3$-type compounds. In particular, three ANN models of estimation of lattice constants a, b and c have been established by APEX tool, and a set of atomic parameters, i.e. ionic radius r, electronegativity x and ionic valance z, are used as the inputs of the ANN models. Subsequently, the models are used to predict the lattice constants of the 'new' compounds of $GdFeO_3$ structure in good agreement with experiments.

2. Factors governing the ionic crystal structure

It is well known that Gibbs free energy determines the stable atomic (ionic) arrangement, i.e. the crystal structure (space-lattice and lattice constant). The general representation of Gibbs free energy is given in Eq. (1) and for crystals in Eq. (2).

$$G = H - TS \tag{1}$$

$$G = U + PV + 1/2h\nu - TS \tag{2}$$

It can be seen from Eq. (2) that the free energy G is the sum of lattice energy U and other terms which are very small at low temperature (T) and pressures (P). In other words, Eq. (2) can be reduced to $G \cong U$ at low T and P, which indicates that the lattice energy determines which structure will form. Born [4] proposed that the interaction of two ions i and j with electric charges $z_i e$ and $z_j e$ can be described with the following equation

$$V_{ij} = Z_i Z_j / r_{ij} + b_{ij} e^2 / r_{ij}^n \tag{3}$$

The total lattice energy is the sum of all V_{ij}, and $r_{ij} = r_i + r_j$. This suggests that the lattice energy of ionic compounds is mainly governed by the radii and valence of its ions. In addition, Electronegativity of ions is another factor affecting the lattice energy. The difference of electronegativity between anion and cation determines the degree of ionic character of bonds; this in turn affects the bond energy and, therefore, the crystal structure. In summary, it seems reasonable to argue that the lattice energy or crystal structure is governed by the radii, valence and electronegativities of the constituent ions.

Based on the above analysis, the lattice constants of the $GdFeO_3$-type ABO_3 may be correlated compounds as a general function of nine variables as below

$$\text{Lattice constant} = f(z_A, z_B, z_O, r_A, r_B, r_O, x_A, x_B, x_O) \tag{4}$$

where z, r and x denote the valence, the radius and the electronegativity of the ion, respectively. It is noted that the three variables associated with anion O^{2-}, namely z_O, r_O, and x_O, can be ignored as they remain unchanged for all samples of our study. Furthermore, there exists a constraint of the valence numbers, i.e. the total valence numbers of anions should be equal to those of cations

$$z_A + z_B = 3 \times z_O = 3 \times 2 = 6 \tag{5}$$

Eq. (5) indicates that the valence of cation A is collinear to that of cation B for these compounds. Thus only valence numbers of one type of cation are independent. In summary, for the lattice constants of the $GdFeO_3$-type compound ABO_3 the general function of Eq. (4) can be reduced as a five-parameter function shown in Eq. (6)

$$\text{Lattice constant} = f(r_A, r_B, x_A, x_B, z_A) \tag{6}$$

Obviously, Eq. (6) represents a multi-variant problem and the function type is usually unknown a prior. Since ANN methods have the intrinsic ability to handle systems involved many variables and relationship that are very complex and poorly understood, it would be advantageous for the present study to use ANN to correlate and predict the lattice constants.

3. Background of ANN

ANN [20] is an information-processing paradigm inspired by the way the densely interconnected, parallel structure of the human brain processes information. The key element of the ANN paradigm is the novel structure of the information processing system. It is composed of a large number of highly interconnected processing elements tied together with weighted connections.

When dealing with certain problems, there are significant advantages of using ANN as compared to conventional computational techniques. These problems include problems with noisy data, problems of pattern recognition, problems where relationships may be dynamic or nonlinear, and problems that an algorithmic solution cannot be formulated [20–22]. The advantages of using ANN in these cases lie in their resilience against distortions in the input data and their capability of learning.

An ANN is comprised of several layers. There is an input layer and an output layer. Between them, there is at least one hidden layer. Each layer consists of several processing elements called nodes. Each node in the hidden layer is fully connected to the inputs. That means what is learnt in a hidden node is based on all the inputs taken together.

An ANN must be trained before it can be used. When the ANN is trained, it is exposed to a set of input and their desired output [23]. The ANN will then organize itself, and adjusts the weights of the connections to cause the overall network to output appropriate results [24]. There are many algorithms for accomplishing this, but they all involve a search for the proper set of weights that will do the best job of accurately predicting the outputs [25]. In the present study, the commonly used back-propagation (BP) [21] network is used.

4. Prediction model of lattice constants

4.1. Collection of the data

It is well known that most perovskites undergo structure transformation with different temperature or pressure [28]. For instance, Barium titante ($BaTiO_3$) has the following transformations

$$\text{Rhombohedral} \overset{-100\ ^\circ\text{C}}{\longrightarrow} \textit{Orthorhombic} \overset{0\ ^\circ\text{C}}{\longrightarrow} \text{tetragonal} \overset{120\ ^\circ\text{C}}{\longrightarrow}$$

$$\text{cubic and lead titanate transforms tetragonal} \overset{490\ ^\circ\text{C}}{\longrightarrow} \text{cubic}$$

Due to phase transitions, lattice constants change in accordance to temperature and pressure. Since the goal of the present study is to investigate the regularities of lattice constants of $GdFeO_3$-type compounds at room temperature and standard atmospheric pressure, unit cell parameters measured under these conditions are accepted.

A total of 161 $GdFeO_3$-type compounds are collected for the present study. Among which, 157 compounds are used for model development. For consistency, lattice constant data at room temperature and standard atmosphere are selected in this study. They are compiled from the following sources: Inorganic Compounds Structural Database (ICSD) [26]; Powder Diffraction File (PDF) [27]; Perovskites and High T_c Superconductors [28] and The Major Ternary Structural Families [4]. The other four compounds are acquired from the most recent publications [29–32] and treated as new compounds. Their lattice constants are predicted by the trained models and compared with the literature data. Estimations of four new compounds may be regarded as additional test of the developed models.

Atomic parameters chosen for this study are acquired from various sources. Ionic radii of most ions are cited from Handbook of Chemistry and Physics [33]. For those unavailable in this handbook, they are collected from Elements [34] and Perovskites and High Tc Superconductors [28]. Electronegativities are obtained from Handbook of Chemistry and Physics.

Table 1 lists all the 157 compounds and their lattice constants a, b and c as well as the set of five atomic parameters of their constituent ions, namely the ionic radii r and electronegativities x of cation A and B, respectively, and the valence z of ion A. The set of the atomic parameters are used as the inputs for developing the ANN models. Similarly in Table 2, the four new compounds are listed and used to test the developed models.

4.2. Linear regression model

Before looking into the complex relationship between lattice constant and atomic properties, a simple linear regression (LR) analysis is conducted. In the following, 157 compounds from Table 1 are used to construct simple LR models.

Based on Eq. (3), ionic radius is expected to strongly govern the lattice constants of ionic compounds. Only two ionic radii or their combinations are used to build simple linear models. Four terms are found efficient in constructing LR models; ionic radius r_A, r_B, tolerance factor $t = (r_A + r_0)/\sqrt{2}(r_B + r_0)$ and r_A/t. Their regression equations for lattice constants a, b and c are

$$a = 17.2443 + 7.5013r_A - 3.2537r_B - 17.4019t - 2.1508(r_A/t)$$

$$R^2 = 0.8851$$

$$b = -2.9248 - 0.1803r_A + 8.2772r_B + 10.7858t - 2.8652(r_A/t)$$

$$R^2 = 0.9029$$

Table 1
Results of the lattice constant (LC) prediction by ANN for the training and validation data set

No	Compound	r		X		z (A)	Citation[a]	Experimental LC (Å)			Model predicted LC (Å)			PAD		
		A	B	A	B			a	b	c	a	b	c	a	b	c
1	$BaCeO_3$	1.35	0.87	0.89	1.12	2	2751	6.235	8.781	6.212	6.2207	8.7216	6.2084	0.23	0.68	0.06
2	$BaPrO_3$	1.35	0.85	0.89	1.13	2	2753	6.214	8.722	6.181	6.1767	8.7392	6.1766	0.60	0.20	0.07
3	$BaPuO_3$	1.35	0.86	0.89	1.3	2	65033	6.193	8.744	6.219	6.205	8.7457	6.1882	0.19	0.02	0.50
4	$CaCrO_3$	1.00	0.55	1	1.66	2	21-0137	5.316	7.486	5.287	5.295	7.4748	5.2871	0.39	0.15	0.00
5	$CaGeO_3$	1.00	0.53	1	2.01	2	31338	5.2688	7.4452	5.2607	5.2853	7.4485	5.2504	0.31	0.04	0.20
6	$CaMnO_3$	1.00	0.53	1	1.55	2	50997	5.2819	7.4547	5.2658	5.2414	7.4552	5.2608	0.77	0.01	0.09
7	$CaRuO_3$	1.00	0.62	1	2.2	2	51291	5.519	7.665	5.364	5.5174	7.732	5.3785	0.03	0.87	0.27
8	$CaSnO_3$	1.00	0.69	1	1.96	2	59160	5.681	7.906	5.532	5.6656	7.9734	5.4942	0.27	0.85	0.68
9	$CaTiO_3$	1.00	0.61	1	1.54	2	88347	5.4537	7.6551	5.3827	5.4332	7.64	5.3794	0.38	0.20	0.06
10	$CaVO_3$	1.00	0.58	1	1.63	2	Muller	5.352	7.547	5.326	5.3641	7.5473	5.3319	0.23	0.00	0.11
11	$CaZrO_3$	1.00	0.72	1	1.33	2	37264	5.7616	8.0171	5.5912	5.7334	8.0003	5.5591	0.49	0.21	0.57
12	$CdTiO_3$	0.95	0.61	1.69	1.54	2	62150	5.4215	7.6176	5.3053	5.3743	7.6267	5.3587	0.87	0.12	1.01
13	$CeVO_3$	1.01	0.64	1.12	1.63	3	63521	5.557	7.808	5.514	5.5655	7.8095	5.5112	0.15	0.02	0.05
14	$CoSeO_3$	0.50	0.65	2.55	1.88	4	496	5.9297	7.5954	5.0293	5.8945	7.578	4.9831	0.59	0.23	0.92
15	$CoTeO_3$	0.97	0.65	2.1	1.88	4	500	6.0169	7.5147	5.3266	5.9944	7.4462	5.3409	0.37	0.91	0.27
16	$DyFeO_3$	0.91	0.65	1.22	1.83	3	27280	5.598	7.623	5.302	5.5927	7.6132	5.3061	0.09	0.13	0.08
17	$DyMnO_3$	0.91	0.65	1.22	1.55	3	Muller	5.828	7.375	5.275	5.841	7.4761	5.31	0.22	1.37	0.66
18	$DyNiO_3$	0.91	0.56	1.22	1.91	3	87803	5.5056	7.4455	5.2063	5.4301	7.5037	5.1968	1.37	0.78	0.18
19	$DyVO_3$	0.91	0.64	1.22	1.63	3	40392	5.598	7.586	5.292	5.5898	7.5805	5.2964	0.15	0.07	0.08
20	$ErFeO_3$	0.89	0.65	1.24	1.83	3	27282	5.582	7.591	5.263	5.5902	7.5755	5.2825	0.15	0.20	0.37
21	$ErVO_3$	0.89	0.64	1.24	1.63	3	40393	5.598	7.5865	5.292	5.6002	7.541	5.2728	0.04	0.60	0.36
22	$EuFeO_3$	0.95	0.65	1.1	1.83	3	27277	5.606	7.685	5.372	5.5939	7.6862	5.3893	0.22	0.02	0.32
23	$EuMnO_3$	0.95	0.65	1.1	1.55	3	26-1126	5.842	7.451	5.336	5.803	7.5606	5.3926	0.67	1.47	1.06
24	$EuNiO_3$	0.95	0.56	1.1	1.91	3	88039	5.4586	7.5371	5.2941	5.4248	7.5513	5.2851	0.62	0.19	0.17
25	$GdFeO_3$	0.94	0.65	1.2	1.83	3	27278	5.611	7.669	5.349	5.5971	7.6849	5.3566	0.25	0.21	0.14
26	$GdNiO_3$	0.94	0.56	1.2	1.91	3	88040	5.4854	7.5112	5.2606	5.431	7.537	5.249	0.99	0.34	0.22
27	$GdTiO_3$	0.94	0.67	1.2	1.54	3	8149	5.691	7.664	5.393	5.695	7.674	5.3851	0.07	0.13	0.15
28	$GdVO_3$	0.94	0.64	1.2	1.63	3	40391	5.62	7.643	5.35	5.5784	7.6674	5.3469	0.74	0.32	0.06
29	$HoFeO_3$	0.89	0.65	1.23	1.83	3	27281	5.591	7.602	5.278	5.5889	7.573	5.282	0.04	0.38	0.08
30	$HoMnO_3$	0.89	0.65	1.23	1.55	3	Muller	5.831	7.354	5.255	5.8249	7.4422	5.286	0.11	1.20	0.59
31	$LaCrO_3$	1.03	0.62	1.1	1.66	3	50755	5.4797	7.7588	5.5163	5.5161	7.7566	5.5174	0.66	0.03	0.02
32	$LaErO_3$	1.03	0.89	1.1	1.24	3	16237	6.07	8.45	5.85	6.0818	8.4713	5.8713	0.19	0.25	0.36
33	$LaFeO_3$	1.03	0.65	1.1	1.83	3	78062	5.5652	7.8543	5.557	5.6084	7.8673	5.5518	0.78	0.17	0.09
34	$LaMnO_3$	1.03	0.65	1.1	1.55	3	90424	5.7478	7.6921	5.5352	5.7723	7.7262	5.5533	0.43	0.44	0.33
35	$LaRuO_3$	1.03	0.68	1.1	2.2	3	75569	5.6847	7.8897	5.5462	5.7421	7.8535	5.5457	1.01	0.46	0.01
36	$LaTiO_3$	1.03	0.67	1.1	1.54	3	Muller	5.753	7.832	5.546	5.7598	7.8049	5.5775	0.12	0.35	0.57
37	$LaTmO_3$	1.03	0.88	1.1	1.25	3	25-1061	6.052	8.429	5.844	6.0598	8.4507	5.8572	0.13	0.26	0.23
38	$LaVO_3$	1.03	0.64	1.1	1.63	3	63520	5.543	7.84	5.543	5.5655	7.8479	5.541	0.41	0.10	0.04
39	$MgSeO_3$	0.50	0.72	2.55	1.31	4	494	5.9246	7.6663	5.0059	5.9081	7.6448	5.0753	0.28	0.28	1.39
40	$MnSeO_3$	0.50	0.83	2.55	1.55	4	495	6.0945	7.8656	5.146	6.1121	7.822	5.1365	0.29	0.55	0.18
41	$MnTeO_3$	0.97	0.83	2.1	1.55	4	29-0900	6.144	7.787	5.441	6.098	7.7646	5.4749	0.75	0.29	0.62
42	$NaIO_3$	1.02	0.95	0.93	2.66	1	202679	6.3953	8.128	5.75	6.3852	8.22	5.7464	0.16	1.13	0.06
43	$NdFeO_3$	0.98	0.65	1.14	1.83	3	78587	5.5835	7.7602	5.4504	5.6007	7.7658	5.4551	0.31	0.07	0.09
44	$NdMnO_3$	0.98	0.65	1.14	1.55	3	15719	5.854	7.557	5.38	5.8184	7.5947	5.458	0.61	0.50	1.45
45	$NdTiO_3$	0.98	0.67	1.14	1.54	3	Muller	5.707	7.765	5.487	5.7158	7.7117	5.4822	0.15	0.69	0.09
46	$NdVO_3$	0.98	0.64	1.14	1.63	3	Muller	5.579	7.734	5.451	5.5682	7.7239	5.4453	0.19	0.13	0.11
47	$NiSeO_3$	0.50	0.69	2.55	1.91	4	497	5.8803	7.5235	4.9394	5.9656	7.595	4.9607	1.45	0.95	0.43
48	$NiTeO_3$	0.97	0.69	2.1	1.91	4	29-0937	5.956	7.499	5.213	5.9408	7.5479	5.2343	0.26	0.65	0.41
49	$PrFeO_3$	0.99	0.65	1.13	1.83	3	63645	5.591	7.783	5.486	5.6022	7.7885	5.4796	0.20	0.07	0.12
50	$PrMnO_3$	0.99	0.65	1.13	1.55	3	Muller	5.787	7.575	5.545	5.8108	7.6161	5.4822	0.41	0.54	1.13
51	$PrNiO_3$	0.99	0.56	1.13	1.91	3	67721	5.4193	7.6263	5.3801	5.4303	7.6267	5.3766	0.20	0.00	0.07
52	$SmAlO_3$	0.96	0.54	1.17	1.61	3	10334	5.291	7.474	5.29	5.3272	7.4312	5.2789	0.68	0.57	0.21
53	$SmFeO_3$	0.96	0.65	1.17	1.83	3	27276	5.597	7.711	5.4	5.5986	7.7245	5.403	0.03	0.18	0.06
54	$SmNiO_3$	0.96	0.56	1.17	1.91	3	90959	5.4289	7.563	5.3268	5.4303	7.5726	5.2974	0.03	0.13	0.55

(*continued on next page*)

Table 1 (*continued*)

No	Compound	*r*		*X*		*z* (A)	Citation[a]	Experimental LC (Å)			Model predicted LC (Å)			PAD		
		A	B	A	B			*a*	*b*	*c*	*a*	*b*	*c*	*a*	*b*	*c*
55	$SmTiO_3$	0.96	0.67	1.17	1.54	3	Muller	5.665	7.737	5.468	5.7052	7.6947	5.4309	0.71	0.55	0.68
56	$SrCeO_3$	1.18	0.87	0.95	1.12	2	78536	6.145	8.575	6	6.1762	8.5514	6.0224	0.51	0.28	0.37
57	$SrHfO_3$	1.18	0.71	0.95	1.3	2	89383	5.7646	8.1344	5.7516	5.7705	8.1237	5.7484	0.10	0.13	0.06
58	$SrOsO_3$	1.18	0.63	0.95	2.2	2	30-1300	5.58	7.9	5.55	5.5871	7.905	5.5907	0.13	0.06	0.73
59	$SrPbO_3$	1.18	0.78	0.95	1.8	2	78682	5.9544	8.3293	5.8627	5.9621	8.4085	5.8533	0.13	0.95	0.16
60	$SrPrO_3$	1.18	0.85	0.95	1.13	2	84882	6.1168	8.5487	5.9857	6.1292	8.5178	5.9889	0.20	0.36	0.05
61	$SrRuO_3$	1.18	0.62	0.95	2.2	2	51292	5.541	7.854	5.574	5.5621	7.8777	5.5743	0.38	0.30	0.00
62	$SrSnO_3$	1.18	0.69	0.95	1.96	2	90845	5.6974	8.0519	5.6986	5.7269	8.1244	5.697	0.52	0.90	0.03
63	$SrZrO_3$	1.18	0.72	0.95	1.33	2	650	5.815	8.196	5.815	5.7943	8.172	5.7644	0.36	0.29	0.87
64	$TbAlO_3$	0.92	0.54	1.1	1.61	3	84422	5.3058	7.4154	5.2296	5.3214	7.4579	5.2017	0.29	0.57	0.53
65	$TbFeO_3$	0.92	0.65	1.1	1.83	3	84412	5.5978	7.6406	5.3268	5.5856	7.6567	5.3256	0.22	0.21	0.02
66	$TbMnO_3$	0.92	0.65	1.1	1.55	3	15720	5.831	7.403	5.297	5.774	7.5376	5.3292	0.98	1.82	0.61
67	$TbVO_3$	0.92	0.64	1.1	1.63	3	25-0818	5.606	7.614	5.325	5.5767	7.5005	5.3161	0.52	1.49	0.17
68	$TmFeO_3$	0.88	0.65	1.25	1.83	3	27283	5.576	7.584	5.251	5.5889	7.5589	5.273	0.23	0.33	0.42
69	$TmVO_3$	0.88	0.64	1.25	1.63	3	25-0899	5.573	7.545	5.237	5.6062	7.5235	5.2633	0.60	0.29	0.50
70	$YbAlO_3$	0.86	0.54	1.1	1.61	3	24-1399	5.331	7.3146	5.1251	5.3157	7.409	5.1174	0.29	1.29	0.15
71	$YbFeO_3$	0.86	0.65	1.1	1.83	3	27284	5.557	7.57	5.233	5.5585	7.6137	5.2431	0.03	0.58	0.19
72	$YbVO_3$	0.86	0.64	1.1	1.63	3	25-1016	5.563	7.533	5.223	5.5811	7.4549	5.2336	0.33	1.04	0.20
73	$YCrO_3$	0.90	0.62	1.22	1.66	3	Muller	5.521	7.532	5.241	5.5116	7.5189	5.2582	0.17	0.17	0.33
74	$YFeO_3$	0.90	0.65	1.22	1.83	3	23011	5.587	7.599	5.279	5.5903	7.5901	5.2931	0.06	0.12	0.27
75	$YTiO_3$	0.90	0.67	1.22	1.54	3	84609	5.6901	7.613	5.3381	5.6587	7.5953	5.3226	0.55	0.23	0.29
76	$PuCrO_3$	1.00	0.62	1.3	1.66	3	Muller	5.51	7.76	5.46	5.5212	7.6672	5.4456	0.20	1.20	0.26
77	$LuCrO_3$	0.86	0.62	1	1.66	3	Muller	5.497	7.475	5.176	5.5176	7.4796	5.2043	0.37	0.06	0.55
78	$YbCrO_3$	0.86	0.62	1.1	1.66	3	Muller	5.51	7.49	5.195	5.5102	7.4025	5.2089	0.08	1.17	0.27
79	$TmCrO_3$	0.88	0.62	1.25	1.66	3	Muller	5.508	7.5	5.209	5.5142	7.5062	5.2378	0.11	0.08	0.55
80	$HoCrO_3$	0.89	0.62	1.23	1.66	3	Muller	5.519	7.538	5.243	5.5124	7.4999	5.247	0.12	0.51	0.08
81	$TbCrO_3$	0.92	0.62	1.1	1.66	3	Muller	5.518	7.576	5.291	5.5097	7.4701	5.2919	0.15	1.40	0.02
82	$EuCrO_3$	0.95	0.62	1.1	1.66	3	Muller	5.515	7.622	5.34	5.5107	7.5528	5.3559	0.08	0.91	0.30
83	$SmCrO_3$	0.96	0.62	1.17	1.66	3	Muller	5.508	7.643	5.367	5.5105	7.6422	5.3692	0.05	0.01	0.04
84	$PmCrO_3$	0.97	0.62	1.1	1.66	3	Muller	5.49	7.69	5.4	5.5118	7.6082	5.4037	0.40	1.06	0.07
85	$CeCrO_3$	1.01	0.62	1.12	1.66	3	Muller	5.475	7.74	5.475	5.5137	7.7243	5.4878	0.71	0.20	0.23
86	$PrCrO_3$	0.99	0.62	1.13	1.66	3	Muller	5.479	7.718	5.448	5.512	7.6758	5.4461	0.60	0.55	0.04
87	$NdCrO_3$	0.98	0.62	1.14	1.66	3	84995	5.4798	7.6918	5.4221	5.5113	7.6591	5.4215	0.57	0.42	0.01
88	$ErCrO_3$	0.89	0.62	1.24	1.66	3	28487	5.516	7.519	5.223	5.5131	7.5242	5.2475	0.05	0.07	0.47
89	$DyCrO_3$	0.91	0.62	1.22	1.66	3	16505	5.525	7.561	5.271	5.5115	7.5589	5.2713	0.24	0.03	0.01
90	$GdCrO_3$	0.94	0.62	1.2	1.66	3	38023	5.515	7.6	5.312	5.5109	7.6272	5.3223	0.08	0.36	0.19
91	$NdNiO_3$	0.98	0.56	1.14	1.91	3	78319	5.4042	7.5991	5.3726	5.43	7.6105	5.3513	0.48	0.15	0.40
92	$PrRuO_3$	0.99	0.68	1.13	2.2	3	75570	5.8344	7.7477	5.3794	5.739	7.7571	5.4746	1.64	0.12	1.77
93	$CeFeO_3$	1.01	0.65	1.12	1.83	3	Muller	5.536	7.819	5.519	5.6052	7.8304	5.5216	1.25	0.15	0.05
94	$HoAlO_3$	0.89	0.54	1.23	1.61	3	39606	5.322	7.374	5.18	5.325	7.3327	5.1531	0.06	0.56	0.52
95	$TmAlO_3$	0.88	0.54	1.25	1.61	3	Muller	5.33	7.29	5.15	5.3259	7.3128	5.1435	0.08	0.31	0.13
96	$LuFeO_3$	0.86	0.65	1	1.83	3	Muller	5.547	7.565	5.213	5.5474	7.591	5.2379	0.01	0.34	0.48
97	$LaRhO_3$	1.03	0.67	1.1	2.28	3	Muller	5.679	7.9	5.524	5.7369	7.8414	5.4768	1.02	0.74	0.85
98	$CeTiO_3$	1.01	0.67	1.12	1.54	3	Muller	5.757	7.801	5.513	5.745	7.7724	5.5477	0.21	0.37	0.63
99	$PrVO_3$	0.99	0.64	1.13	1.63	3	Muller	5.562	7.751	5.487	5.5671	7.7478	5.4697	0.09	0.04	0.32
100	$PrRhO_3$	0.99	0.67	1.13	2.28	3	Muller	5.747	7.803	5.414	5.7344	7.7774	5.4087	0.22	0.33	0.10
101	$PrTiO_3$	0.99	0.67	1.13	1.54	3	Muller	5.724	7.798	5.499	5.7238	7.7271	5.5063	0.00	0.91	0.13
102	$NdRhO_3$	0.98	0.67	1.14	2.28	3	Muller	5.755	7.774	5.378	5.734	7.759	5.3858	0.37	0.19	0.15
103	$SmVO_3$	0.96	0.64	1.17	1.63	3	Muller	5.588	7.672	5.393	5.5721	7.6974	5.3934	0.28	0.33	0.01
104	$SmMnO_3$	0.96	0.65	1.17	1.55	3	Muller	5.843	7.482	5.359	5.8337	7.5642	5.4064	0.16	1.10	0.88
105	$SmRhO_3$	0.96	0.67	1.17	2.28	3	Muller	5.761	7.708	5.321	5.7341	7.7242	5.3394	0.47	0.21	0.35
106	$EuRhO_3$	0.95	0.67	1.1	2.28	3	Muller	5.761	7.68	5.298	5.7293	7.6682	5.3096	0.55	0.15	0.22
107	$GdMnO_3$	0.94	0.65	1.2	1.55	3	Muller	5.853	7.432	5.313	5.8462	7.5396	5.3602	0.12	1.45	0.89
108	$GdRhO_3$	0.94	0.67	1.2	2.28	3	Muller	5.761	7.658	5.277	5.7347	7.6921	5.2986	0.46	0.45	0.41
109	$TbRhO_3$	0.92	0.67	1.1	2.28	3	Muller	5.749	7.623	5.254	5.7264	7.6341	5.2451	0.39	0.15	0.17

(*continued on next page*)

Table 1 (*continued*)

No	Compound	*r*		*X*		*z* (A)	Citation[a]	Experimental LC (Å)			Model predicted LC (Å)			PAD		
		A	B	A	B			*a*	*b*	*c*	*a*	*b*	*c*	*a*	*b*	*c*
110	$TbTiO_3$	0.92	0.67	1.1	1.54	3	Muller	5.648	7.676	5.388	5.6417	7.5928	5.3538	0.11	1.08	0.63
111	$DyRhO_3$	0.91	0.67	1.22	2.28	3	Muller	5.731	7.6	5.245	5.7338	7.6299	5.2514	0.05	0.39	0.12
112	$DyTiO_3$	0.91	0.67	1.22	1.54	3	Muller	5.659	7.647	5.361	5.6691	7.6228	5.3354	0.18	0.32	0.48
113	$HoRhO_3$	0.89	0.67	1.23	2.28	3	Muller	5.726	7.582	5.23	5.733	7.587	5.2286	0.12	0.07	0.03
114	$HoTiO_3$	0.89	0.67	1.23	1.54	3	Muller	5.665	7.626	5.339	5.653	7.5822	5.3117	0.21	0.57	0.51
115	$ErRhO_3$	0.89	0.67	1.24	2.28	3	Muller	5.712	7.561	5.216	5.734	7.5944	5.231	0.38	0.44	0.29
116	$ErTiO_3$	0.89	0.67	1.24	1.54	3	Muller	5.657	7.613	5.318	5.6569	7.5967	5.3123	0.00	0.21	0.11
117	$TmTiO_3$	0.88	0.67	1.25	1.54	3	Muller	5.647	7.607	5.306	5.6514	7.5842	5.303	0.08	0.30	0.06
118	$YbTiO_3$	0.86	0.67	1.1	1.54	3	Muller	5.633	7.598	5.293	5.6111	7.5501	5.2723	0.39	0.63	0.39
119	$LuTiO_3$	0.86	0.67	1	1.54	3	Muller	5.633	7.58	5.274	5.625	7.6242	5.2663	0.14	0.58	0.15
120	YVO_3	0.90	0.64	1.22	1.63	3	Muller	5.605	7.587	5.284	5.5937	7.5402	5.2834	0.20	0.62	0.01
121	$YMnO_3$	0.90	0.65	1.22	1.55	3	Muller	5.83	7.36	5.26	5.8303	7.4561	5.297	0.00	1.31	0.70
122	$AmVO_3$	0.98	0.64	0.89	1.63	3	Muller	5.58	7.76	5.45	5.6057	7.6923	5.4695	0.46	0.87	0.36
123	$PuVO_3$	1.00	0.64	1.3	1.63	3	Muller	5.61	7.78	5.48	5.5718	7.7204	5.4701	0.68	0.77	0.18
124	$LaScO_3$	1.03	0.75	1.1	1.36	3	Muller	5.787	8.098	5.678	5.7715	8.0917	5.6799	0.27	0.08	0.03
125	$LaInO_3$	1.03	0.80	1.1	1.78	3	Muller	5.914	8.207	5.723	5.9204	8.173	5.7368	0.11	0.41	0.24
126	$LaLuO_3$	1.03	0.86	1.1	1	3	Muller	6.009	8.385	5.824	6.0072	8.3788	5.832	0.03	0.07	0.14
127	$PrCoO_3$	0.99	0.55	1.13	1.88	3	Muller	5.373	7.587	5.331	5.4031	7.5696	5.3661	0.56	0.23	0.66
128	$PrScO_3$	0.99	0.75	1.13	1.36	3	Muller	5.776	8.027	5.615	5.7574	8.0451	5.6079	0.32	0.23	0.13
129	$PrLuO_3$	0.99	0.86	1.13	1	3	Muller	5.977	8.32	5.751	5.9798	8.3155	5.7572	0.05	0.05	0.11
130	$NdCoO_3$	0.98	0.55	1.14	1.88	3	Muller	5.336	7.547	5.336	5.4028	7.5529	5.3408	1.25	0.08	0.09
131	$NdScO_3$	0.98	0.75	1.14	1.36	3	Muller	5.771	7.998	5.574	5.7537	8.0319	5.5842	0.30	0.42	0.18
132	$NdInO_3$	0.98	0.80	1.14	1.78	3	Muller	5.891	8.121	5.627	5.9113	8.1096	5.6395	0.35	0.14	0.22
133	$PmScO_3$	0.97	0.75	1.1	1.36	3	Muller	5.79	7.94	5.56	5.7643	7.9857	5.5656	0.44	0.58	0.10
134	$PmInO_3$	0.97	0.80	1.1	1.78	3	Muller	5.9	8.2	5.7	5.9194	8.1323	5.62	0.33	0.83	1.40
135	$SmCoO_3$	0.96	0.55	1.17	1.88	3	Muller	5.354	7.541	5.289	5.4031	7.5303	5.2867	0.92	0.14	0.04
136	$SmScO_3$	0.96	0.75	1.17	1.36	3	Muller	5.76	7.95	5.53	5.7451	8.0009	5.5343	0.26	0.64	0.08
137	$SmInO_3$	0.96	0.80	1.17	1.78	3	Muller	5.886	8.082	5.589	5.9063	8.0732	5.5902	0.35	0.11	0.02
138	$EuScO_3$	0.95	0.75	1.1	1.36	3	Muller	5.76	7.94	5.51	5.7618	7.9275	5.5193	0.03	0.16	0.17
139	$GdCoO_3$	0.94	0.55	1.2	1.88	3	Muller	5.404	7.436	5.228	5.4038	7.5057	5.2382	0.00	0.94	0.19
140	$GdScO_3$	0.94	0.75	1.2	1.36	3	Muller	5.756	7.925	5.487	5.7385	7.9678	5.4903	0.30	0.54	0.06
141	$DyScO_3$	0.91	0.75	1.22	1.36	3	Muller	5.71	7.89	5.43	5.7333	7.9314	5.4428	0.41	0.52	0.24
142	$HoScO_3$	0.89	0.75	1.23	1.36	3	Muller	5.71	7.87	5.42	5.7304	7.9077	5.4205	0.36	0.48	0.01
143	$YScO_3$	0.86	0.75	1.22	1.36	3	Muller	5.721	7.894	5.431	5.7281	7.8472	5.3924	0.12	0.59	0.71
144	$LaYbO_3$	1.03	0.86	1.1	1.33	3	Muller	6.028	8.402	5.838	6.0182	8.3971	5.8286	0.16	0.06	0.16
145	$LaHoO_3$	1.03	0.89	1.1	1.23	3	Muller	6.092	8.48	5.888	6.0816	8.4727	5.8714	0.17	0.09	0.28
146	$LaYO_3$	1.03	0.90	1.1	1.22	3	Muller	6.087	8.493	5.877	6.1037	8.4922	5.8855	0.27	0.01	0.15
147	$CaMoO_3$	1.00	0.65	1	2.16	2	Muller	5.58	7.8	5.45	5.5848	7.8242	5.4259	0.09	0.31	0.44
148	$CaNbO_3$	1.00	0.68	1	1.6	2	51202	5.6525	7.914	5.5323	5.6186	7.9242	5.4874	0.60	0.13	0.81
149	$CaHfO_3$	1.00	0.71	1	1.3	2	Muller	5.732	7.984	5.568	5.7519	7.977	5.5435	0.35	0.09	0.44
150	$CaUO_3$	1.00	0.89	1	1.7	2	Muller	5.97	8.29	5.78	5.9743	8.3019	5.8337	0.07	0.14	0.93
151	$CdSnO_3$	0.95	0.69	1.69	1.96	2	Muller	5.577	7.867	5.547	5.6308	7.83	5.4734	0.97	0.47	1.33
152	$BaPbO_3$	1.35	0.78	0.89	1.8	2	Muller	6.065	8.506	6.024	6.0417	8.5305	6.0461	0.38	0.29	0.37
153	$SrIrO_3$	1.18	0.63	0.95	2.2	2	Muller	5.6	7.89	5.58	5.5871	7.905	5.5907	0.23	0.19	0.19
154	$NaTaO_3$	1.02	0.64	0.93	1.5	1	Muller	5.513	7.751	5.494	5.5754	7.7687	5.5509	1.13	0.23	1.04
155	$NaNbO_3$	1.02	0.64	0.93	1.6	1	Muller	5.57	7.77	5.51	5.5791	7.7554	5.5483	0.16	0.19	0.70
156	$NaUO_3$	1.02	0.76	0.93	1.7	1	Muller	5.905	8.25	5.775	5.8897	8.1884	5.7453	0.26	0.75	0.51
157	$NaPaO_3$	1.02	0.78	0.93	1.5	1	Muller	5.97	8.36	5.82	5.92	8.2528	5.7845	0.84	1.28	0.61

[a] Notation of the column: Muller refers to Ref. [4] and the codes without/with the hyphens indicate the collection codes in Ref. [27] (PDF) and Ref. [26] (ICSD), respectively.

Table 2
Results of the lattice constant prediction by ANN for the four new compounds

No.	Compound	r		x		z (A)	Experimental LC (Å)			Model predicted LC (Å)			PAD		
		A	B	A	B		a	b	c	a	b	c	a	b	c
1	$SrNbO_3$	1.18	0.68	0.95	1.60	2	5.6944	8.0864	5.6894	5.6885	8.1558	5.6898	0.10	0.86	0.01
2	$CaFeO_3$	1.00	0.59	1.00	1.83	2	5.352	7.539	5.326	5.4043	7.5811	5.3421	0.98	0.56	0.30
3	$TlNiO_3$	0.89	0.56	1.80	1.91	3	5.3677	7.562	5.2549	5.5079	7.3659	5.2146	2.61	2.59	0.77
4	$TlFeO_3$	0.89	0.65	1.80	1.83	3	5.4465	7.7927	5.3172	5.6728	7.5864	5.3361	4.15	2.65	0.36

$$c = -1.4013 - 0.2280r_A + 4.2506r_B + 6.3082t - 0.7542(r_A/t)$$

$$R^2 = 0.9333$$

Where R^2 is the coefficient of determination, which compares estimated and actual values and ranges in value from 0 to 1. Although linear models catch the general trend in lattice constant, they may not be accurate enough for material design research (Table 3). Here, Percentage of the Absolute Difference (PAD) is defined as the ratio of absolute difference between experimental and predicted values over the experimental value. More improvements are necessary.

4.3. Building of prediction ANN model

Besides, we also build non-linear models of ANN including three additional atomic properties. The models are established by the Neural Network Model Builder (NNMB) of an artificial intelligence expert system—Advanced Process Expert (APEX) which was developed in-house on the IBM SP2 supercomputer of the Institute of High Performance Computing. NNMB is a software program used to build models that predict a response (output) variable. It takes the advantage of multiple nodes on the IBM SP2 using a simple task-oriented form of parallelism and, therefore, can build and test multiple neural network models. NNMB was written in Fortran and MATLAB which employs an NN toolbox function to train feed-forward network with Levenberg–Marquardt algorithm.

Table 3
Summary of the percentage of the absolute difference (PAD%) for linear models

LC	a	b	c
Average	0.93	0.82	0.77
Max	3.96	5.61	4.66
Min	0.00	0.00	0.00
Standard deviation	0.83	0.96	0.76

The schematic diagram of the ANN used in the present work is shown in Fig. 1 and it is common to all of the three models. For each of the model, the activation function used in hidden and output layers are chosen as 'tansig' and 'pure linear', respectively; and four neurons are set for all the models. The response variables in the three models are lattice constants a, b, and c, respectively. The five above-mentioned atomic parameters are the input (predictor) variables and they are common to all of the three models. In each model, a randomly selected 90% of the samples are used for model training and the rest for model validation.

5. Results

The results of the lattice constant prediction are presented in Table 1, together with the input atomic parameters and the experimental lattice constants reported in the literature. The accuracy of the ANN model prediction is examined by comparing the experimental with the predicted values of the lattice constants. The analysis of

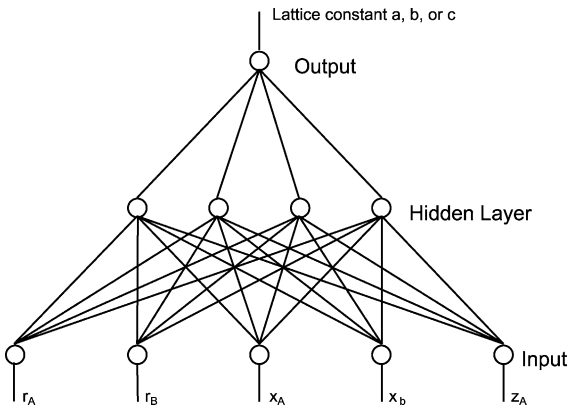

Fig. 1. ANN used for the study of lattice constant of $GdFeO_3$-tpe perovskite.

Table 4
Summary of the percentage of the absolute difference (PAD%) for ANN models

LC	*a*	*b*	*c*
Average	0.35	0.44	0.34
Max	1.64	1.82	1.77
Min	0.00	0.00	0.00
Standard Deviation	0.32	0.39	0.34

the PAD for the three models of the prediction of lattice constants a, b and c is summarized in Table 4.

As can be seen from Table 4, for models of lattice constants a, b and c, the average of PAD are 0.35, 0.44 and 0.34%, and the standard deviation of the PAD are 0.32, 0.39 and 0.34%, respectively. Therefore, it can be concluded that the developed ANN models are fairly accurate and able to well predict the lattice constants due to lower average PAD (less than 1%) and smaller standard deviations of PAD.

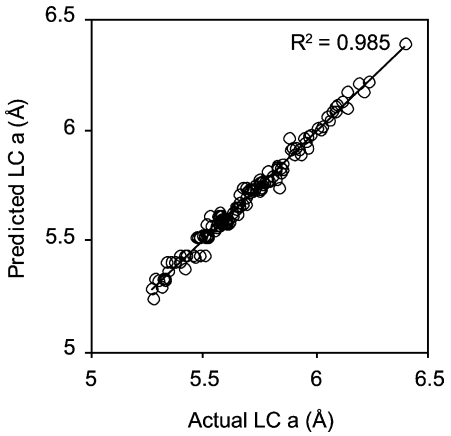

Fig. 2. Lattice constant a (Å) (actual vs. predicted).

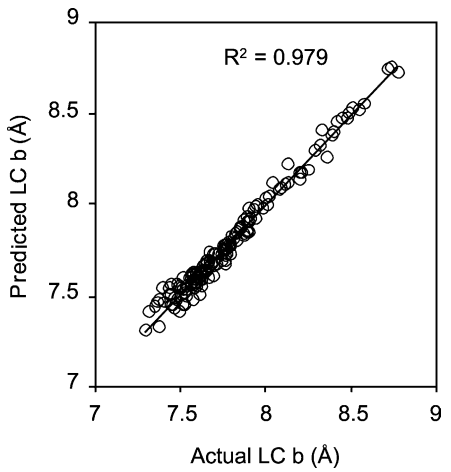

Fig. 3. Lattice constant b (Å) (actual vs. predicted).

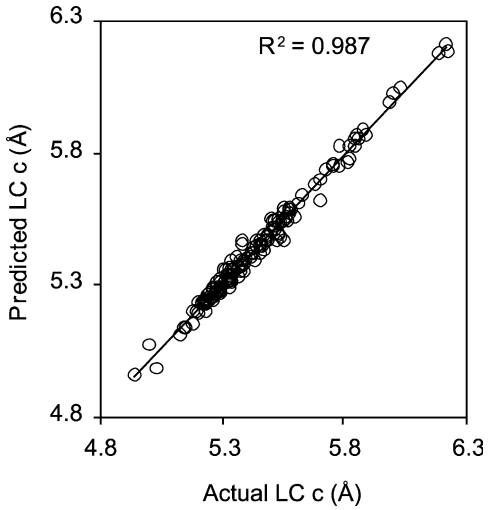

Fig. 4. Lattice constant c (Å) (actual vs. predicted).

The resulting estimates of the lattice constants a, b and c are plotted versus the corresponding experimental values in Figs. 2–4, respectively, for visual examination. It is observed in the three figures that all the data points (actual versus predicted LC values) almost fall in the straight lines of 45°. Further examination of the three trendlines shows that the R^2 values are 0.985, 0.979 and 0.987, respectively, which are very close to 1 indicating that the predicted LC values are in a very good agreement with those from the experimental measurements.

Subsequently, the ANN models are further examined by using a data set of four new ABO_3 compounds that were recently reported. The model inputs, i.e. the predictor variables, are the same as those for model training, namely radii (Å) of ion A and B, electronegativity of ions A and B, and valence electron of ion A. The result is presented in Table 2 in comparison with the values that are extracted from literature [29–32].

6. Discussion

As shown in Table 2, the model of lattice c resulted in excellent estimation since all the PAD values are less than 1%. The model of lattice b also generates acceptable estimation where two PAD values are close to 1% and the other two around 2.6%. On the other hand, the model of lattice a produces very good estimates for most compounds but a few, e.g. $TlFeO_3$ and $TlNiO_3$. Actually $TlNiO_3$ is synthesized [31] at 7.5 GPa and about 700 °C, which deviated far from the room temperature and standard atmosphere condition. For $TlFeO_3$, it is reported [32] that its cell parameters considerably deviate from a trend

observed in the rare earth orthoferrites, which are attributed to a specific coordination of Tl^{3+} ion. Our models may not predict well for the Tl^{3+} containing perovskites. Nevertheless, the three models are quite accurate in general for lattice constant prediction of the $GdFeO_3$ type perovskites.

In the design of new substrate materials or buffer materials for semiconductor epitaxy, lattice mismatch between materials of different layers is one of the main concerns [2,7]. The developed models may provide helpful screening techniques that can rapidly evaluate lattice constants of all possible combinations of elements.

7. Conclusion

In this study, a total number of 157 $GdFeO_3$-type perovskites ABO_3 are collected and used to investigate the regularities of lattice constants. ANN models of a BP neural network are established. Five atomic parameters are selected as the ANN's inputs, namely ionic radii and electronegativities of cation A and B, respectively, and the valence of ion A. Then the lattice constants a, b and c of four Å new compounds are used to further test the ANN models. The following conclusions are obtained

1. Three models of the BP network using five atomic properties have well reproduced measured lattice constants of 157 $GdFeO_3$-type perovskite, with average errors of 0.35, 0.44 and 0.34% for lattice constants a, b and c, respectively.
2. The trained ANN models are also tested using four new compounds, with fairly good agreement, i.e. the average predicted errors are 1.96, 1.66 and 0.36% for lattice constant a, b, and c, respectively.
3. This atomic parameter—ANN technique may provide an alternative to quickly screen a large number of unknown compounds for candidates of a specific lattice constant, which is important to the design of new substrate or buffer materials of semiconductors epitaxy.

References

[1] M.W. Lufaso, P.M. Woodward, Prediction of the crystal structures of perovskites using the software program SpuDS, Acta Cryst. B57 (2001) 725–738.

[2] K. Eisenbeiser, R. Emrickm, R. Droopad, Z. Yu, J. Finder, S. Rockwell, J. Holmes, C. Overgaard, W. Ooms, GaAs MESFETs fabricated on Si substrates using a $SrTiO_3$ buffer layer, IEEE Electr. Device 23 (6) (2002) 300–302.

[3] P.M. Woodward, Octahedral tilting in perovskites. 1. Geometrical considerations, Acta Cryst. B53 (1997) 32–43.

[4] O. Muller, R. Roy, The Major Ternary Structural Families, Springer-Verlag, New York, 1974.

[5] L. Liu, J.H. Edgar, Substrates for gallium nitride epitaxy, Mater. Sci. Engng. R37 (2002) 61–127.

[6] J.I. Langford, D. Louer, Powder diffraction, Pre. Prog. Phys. 59 (1996) 131–234.

[7] V.V. Chernyshev, Structure determination from powder diffraction, Russ. Chem. Bull. Int. Ed. 50 (12) (2001) 2273–2292.

[8] P. Wu, R. Straghan, I. Ong, K.L. Heng, Development of a process diagnosis and optimisation tool for industrial process—a pattern recognition/neural networks code on NSRC's IBM SP2, Proc. IPMM'97, Gold Coast, Australia (1997).

[9] C.H. Li, D.S. Kang, P. Qin, N.Y. Chen, On the stability of Laves phases, T. Nonferr. Metal Soc. 5 (3) (1995) 34.

[10] N.Y. Chen, C.H. Li, S.W. Yao, X.Y. Wang, Regularities of melting behavior of some binary alloy phases.1. Criteria for congruent and incongruent melting, J. Alloys Compd. 234 (1) (1996) 125–129.

[11] C.H. Li, J. Guo, P. Qin, et al., Some regularities of melting points of AB-type intermetallic compounds, J. Phys. Chem. Solids 57 (12) (1996) 1797.

[12] B. Tang, P. Qin, M.X. Liu, N.Y. Chen, Prediction of intermediate compounds in binary halide system, Acta Metal Sinica 30 (1994) 22.

[13] C.H. Li, P. Qin, N.Y. Chen, et al. Proceedings of Expert system for complex halides, 5th China–Japan Bilateral Conference on Molten Salt Chemical and Technology, Kunming (China) 5, 1994, p. 156.

[14] Y.Z. Zeng, S.J. Chua, P. Wu, On the prediction of ternary semiconductor properties by artificial intelligence methods, Chem. Mater. 14 (7) (2002) 2989–2998.

[15] K.L. Heng, S.J. Chua, P. Wu, Prediction of semiconductor material properties by the properties of their constituent chemical elements, Chem. Mater. 12 (6) (2000) 1648–1653.

[16] P. Wu, K.L. Heng, Correlation of chemical element properties to electrochemical properties of hydrogen storage alloys, Chem. Mater. 11 (4) (1999) 858.

[17] K.L. Heng, H.M. Jin, Y. Li, et al., Computer aided design of NiMH electrodes, J. Mater. Chem. 9 (3) (1999) 837–843.

[18] P. Wu, H.M. Jin, Y. Li, Relationship among chemical element properties, bulk additive properties, and crystal structures of binary zinc compounds, Chem. Mater. 11 (11) (1999) 3166–3170.

[19] H.M. Jin, Y. Li, P. Wu, Prediction of new additives for galvanizing process by the properties of their constituent chemical elements, J. Mater.Res. 14 (5) (1999) 1791–1795.

[20] http://www.emsl.pnl.gov:2080/proj/neuron/neural/what.html

[21] http://blizzard.gis.uiuc.edu/htmldocs/neural/neural.html

[22] R.J. Schalkoff, Artificial Neural Networks, McGraw-Hill, New York, 1997, p. 6.

[23] Robert J. Schalkoff, Artificial Neural Networks, McGraw-Hill, New York, 1997, p. 22.

[24] http://hem.hj.se/~de96klda/neuralnetworks.htm

[25] http://www.zsolutions.com/light.htm

[26] Inorganic Crystal Structure Database (ICSD), CD-ROM, version 2002, FIZ Karlsruhe, Fachinformationszentrum Karlsruhe, 76344 Eggenstein-Leopoldshafen, Germany.

[27] Powder diffraction file [electronic resource]: PDF-2database, Newtown Square, Pa., International Centre for Diffraction Data, Version 2002.

[28] F.S. Galasso, Perovskites and High T_c Superconductors, Gordon & Breach Science Publishers, Berlin, 1990.
[29] H. Hannerz, G. Svensson, S.Y. Istomin, O.G. D'yachenko, Transmission electron microscopy and neutron powder diffraction studies of $GdFeO_3$ type $SrNbO_3$, J. Solid State. Chem. 147 (2) (1999) 421–428.
[30] P.M. Woodward, D.E. Cox, E. Moshopoulou, A.W. Sleight, S. Morimoto, Structural studies of charge disproportionation and magnetic order in $CaFeO_3$, Phys. Rev. B62 (2) (2000) 844.
[31] S.J. Kim, G. Demazeau, J.A. Alonso, J.H. Choy, High pressure synthesis and crystal structure of a new Ni(III) perovskite: $TlNiO_3$, J. Mater. Chem. 11 (2001) 487–492.
[32] S.J. Kim, G. Demazeau, I. Presniakov, J.H. Choy, Structural distortion and chemical bonding in $TlFeO_3$: Comparison with AFeO(3) (A = rare earth), J. Solid State Chem. 161 (2) (2001) 197–204.
[33] D.R. Lide, Handbook of Chemistry and Physics, CRC Press/Chapman and Hall, Boca Raton, FL/London, 1999.
[34] J. Emsley, The Elements, Claredon Press, Oxford, 2001.